P12.8 **SYNOPTIC ENVIRONMENTS ASSOCIATED WITH TORNADOES IN NORTHERN ARIZONA**

David O. Blanchard*
NOAA/National Weather Service
Flagstaff, AZ 86015

## 1. INTRODUCTION

Recent tornadic weather events in northern Arizona have exhibited similar synoptic and thermodynamic characteristics suggesting that there may be recurring patterns that can be gleaned from the historical data and which would be beneficial for forecasting future events. A recent event documented by Blanchard (2006) revealed an environment with small buoyant instability, as determined by the convective available potential energy (CAPE), but both large deep-layer and low-level shear. A second, more recent, event also exhibited large shear and small values of CAPE. Moreover, both events occurred when an upper-level closed low moved across Arizona.

The similarities of these two events have motivated this investigation of synoptic environments associated with tornadoes in northern Arizona.

The historical database for the period 1950–2006 was examined and revealed 75 tornado days occurring over northern Arizona[1]. These events were then stratified so that tornadoes occurring during the warm season North American Monsoon (Adams and Comrie 1997) were eliminated since the lack of baroclinity and deep-layer shear generally precludes the development of supercell thunderstorms; instead, non-mesocyclone, non-supercell storms are typical during this regime. The reduced dataset consisted of 38 tornado days.

Inspection of basic synoptic patterns for these events was achieved using the NCEP/NCAR Reanalysis data (Kalnay and Coauthors 1996). Geopotential height, isobaric wind fields, mean sea level pressure, relative humidity, vertical velocity, vertical wind shear, and buoyant instability were assessed using this data.

Additional analysis of the environment was accomplished using the North American radiosonde database (Schwartz and Govett 1992) to more fully analyze shear and instability.

## 2. RESULTS

The basic synoptic patterns for each of the 38 cool-season tornado days were examined using the NCEP/NCAR Reanalysis data. These data show that one half (19/38) of the tornado days occurred during the approach of a mid-tropospheric (i.e., ~700–300 mb) Pacific closed low embedded in the mid-latitude westerlies with northern Arizona located in the warm sector of the low (Fig. A1, Appendix). Although there were variations in the location, strength, and orientation of the low, the similarities among these events were striking. The remaining events encompassed an assortment of synoptic patterns; examination of the residual events is beyond the scope of the current work but will be considered in future analyses.

The next step was to combine the NCEP/NCAR Reanalysis data for each of these 19 cool-season, closed-low events and produce composite fields.

Figure 1 shows the composite 500-mb geopotential height field for all 19 events. Even with the variations between individual events, the structure of the approaching closed low is apparent. The *v*-component of the wind at 850 mb (not shown) and 700 mb (Fig. 2) shows a strong southerly component of the wind which is necessary for advecting warm and, more importantly, moist subtropical air northward across Arizona. Buoyant instability, as revealed by the composite surface-based Lifted Index, is shown in Figure 3. Note that the Lifted Index indicates only marginal instability with most unstable values of only about -1°C.

Upper air soundings from northern Arizona radiosonde sites for these 19 events were examined. The upper air site at Winslow (KINW) was moved to Flagstaff (KFGZ) in 1996 but for the work here is treated as one site. Soundings were not available for all of the events so the total number of soundings is less than the number of events.

[1] There are extended periods of many years with no reported tornado events. While it is possible that these gaps are meteorological in nature, it is more likely that differences in reporting procedures are responsible. Thus, the number of tornado days is almost certainly an undercount.

* *Corresponding author address:* David O. Blanchard, NOAA/NWS, P.O. Box 16057, Flagstaff, AZ 86015; e-mail: david.o.blanchard@noaa.gov.

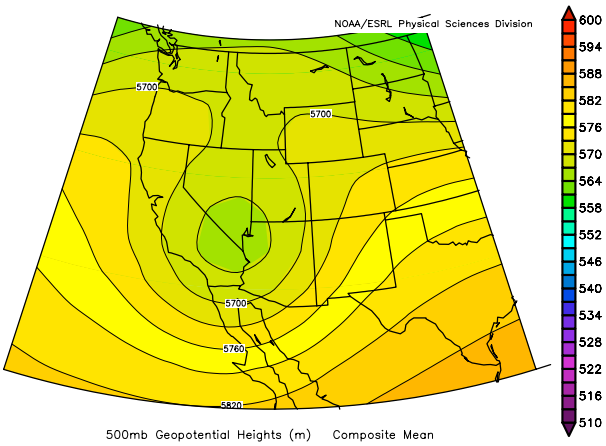


*Figure 1. Composite 500-mb height field for the 19 tornado event days.*

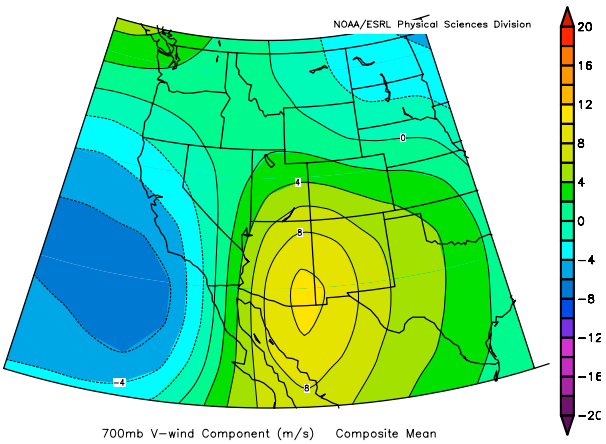


*Figure 2. Composite 700-mb v-component of the wind field.*

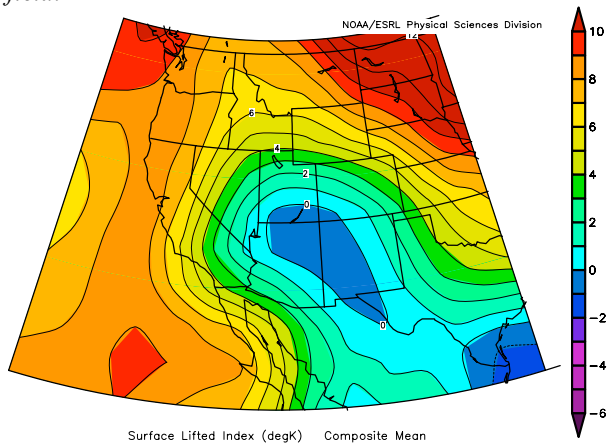


*Figure 3. Composite surface-based Lifted Index field.*

Figure 4 is a box plot and shows the distribution of CAPE for these events. The box encloses 50% of the data with the median shown as a horizontal black line. The top and bottom of the box mark the limits of the 25th and 75th percentiles, respectively, of the variable population. The lines extending from the top and bottom of each box mark the minimum and maximum values within the data set. These are small values of CAPE with a median of ~450 J $kg^{-1}$ (Min/Max values are ~20 J $kg^{-1}$ and ~1200 J $kg^{-1}$, respectively). These values compare to the 1st quartile of tornadic environments discussed by Rasmussen and Blanchard (1998; hereinafter RB98). In fact, these CAPE values are even smaller than the ordinary storm environments discussed by RB98.

The approach of these low-pressure systems typically results in strengthening winds aloft and increasing shear across the region. The Mean Shear in the 0–4 km layer ($MSHR_{0-4}$) is shown in Fig. 5. Mean shear (Rasmussen and Wilhelmson 1983; RB98) is defined as the length of the hodograph divided by the depth over which the hodograph was measured. Median values are ~$7.5x10^{-3}$ $s^{-1}$ (Min/Max values are $0.4x10^{-3}$ $s^{-1}$ and $17.4x10^{-3}$ $s^{-1}$, respectively). This compares favorably with the tornadic environments discussed by RB98.

The magnitude of the bulk shear vector between the 0–500 m AGL mean wind and 6 km AGL wind ($BSHR_{0-6}$) is shown in Fig. 6. The median value of 23 m $s^{-1}$ (Min/Max values are 11 m $s^{-1}$ and 21 m $s^{-1}$, respectively) compares with the 3rd and 4th quartiles of tornadic environments in RB98.

Figure 7 reveals the distribution of the Vorticity Generation Parameter (VGP; RB98). The median value is 0.12 $s^{-1}$ (Min/Max values are 0.0 $s^{-1}$ and 0.26 $s^{-1}$, respectively). This compares to the 1st and 2nd quartiles of RB98 for tornado environments. These values are low since VGP is a product of the $MSHR_{0-4}$ and the square root of CAPE—and CAPE values have already been shown to be marginal for these events. Thus, this parameter, which has been shown to signal which environments are supportive of tornadic supercells in RB98 fails for these events because of the marginal buoyant instability.

Accompanying the deep-layer shear are regions of large 0–3 km Storm Relative Helicity ($SRH_{0-3}$; Fig. 8). The median value for $SRH_{0-3}$ is 112 $m^2$ $s^{-2}$ (Min/Max values are 20 $m^2$ $s^{-2}$ and 302 $m^2$ $s^{-2}$, respectively). This compares favorably with the results shown for supercell and tornado environments by RB98.

Finally, Figs. 9–10 show two representative examples of soundings taken prior to tornadic events in northern Arizona in recent years. Both exhibit strong winds and shear but only marginal instability, and are consistent with the composite results. These are similar to the Miller "Type III" soundings (Miller 1972; Bluestein 1993, p. 453).

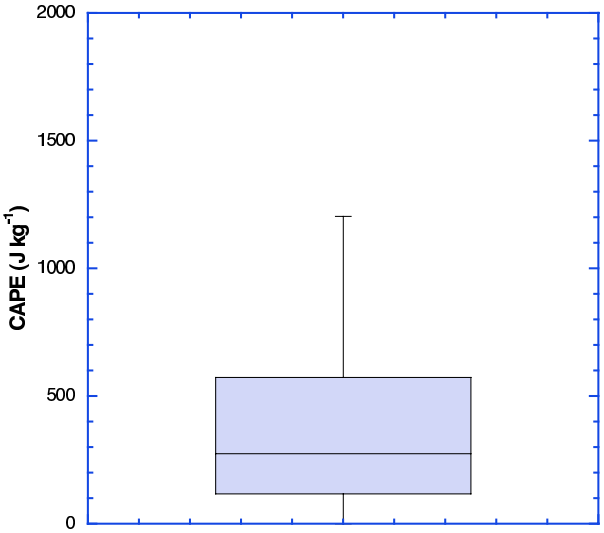


*Figure 4. Box plot showing CAPE (J kg$^{-1}$) distribution for tornado event days.*

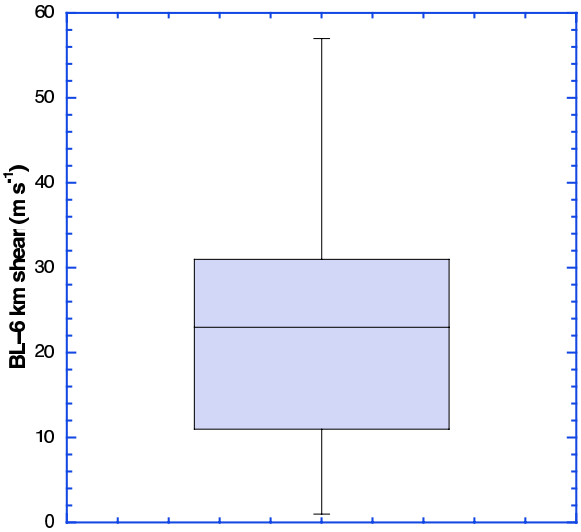


*Figure 6. As in Fig. 4, except for the BL–6-km shear (m s$^{-1}$).*

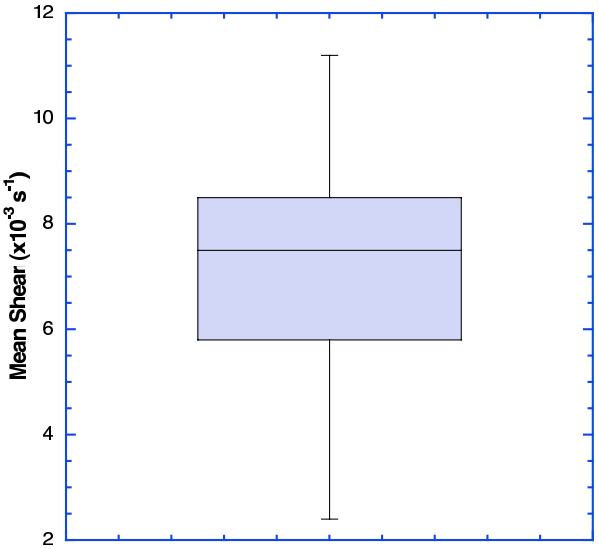


*Figure 5. As in Fig. 4, except for Mean Shear (x10$^{-3}$ s$^{-1}$) in the 0–4 km layer.*

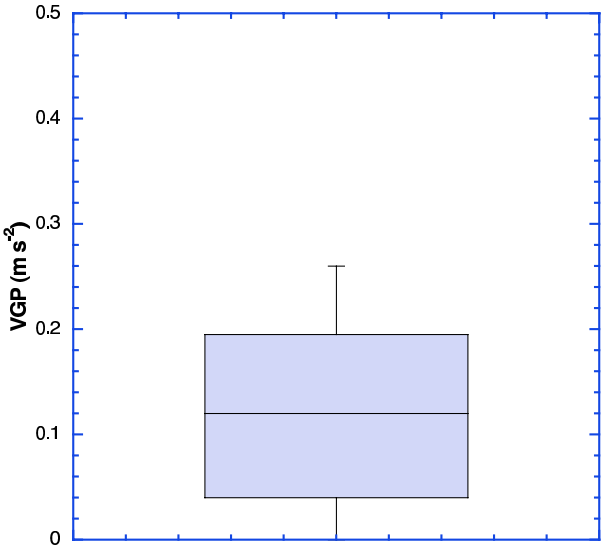


*Figure 7. As in Fig. 4, except for VGP (m s$^{-2}$).*

## 3. DISCUSSION

Recent tornado events occurring in northern Arizona have exhibited strikingly similar synoptic and thermodynamic features. The similarity has prompted this initial examination of the climatology of environments that are responsible for producing tornadoes.

Examination of the synoptic environment indicated that half of the cool-season tornadic days (19/38) were associated with the approach of a closed low from the eastern Pacific with Arizona located in the warm sector of the low. The proximity of a synoptic closed low is similar to results obtained by Hales (1985) for cool-season tornadoes occurring in the Los Angeles Basin in southern California.

Distribution of sounding parameters for the events show that CAPE—and composite parameters based on CAPE—does not compare favorably with the results presented in RB98. The present results all revealed substantially smaller CAPE than the supercell and tornadic environments of RB98.

On the other hand, values for the environmental shear (e.g., SRH, Mean Shear, and Bulk Shear) are large and

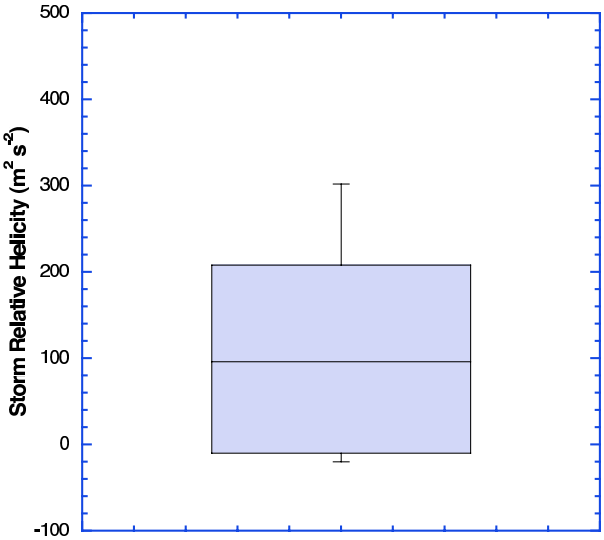


*Figure 8. As in Fig. 4, except for Storm Relative Helicity ($m^2$ $s^{-2}$) for the 0–3 km layer.*

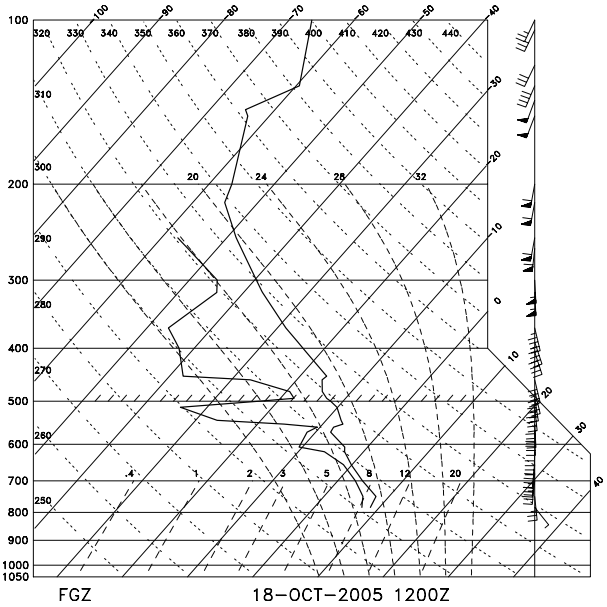


*Figure 9. Skew-T ln p thermodynamic diagram from KFGZ (Flagstaff, AZ) at 1200 UTC 18 October 2005.*

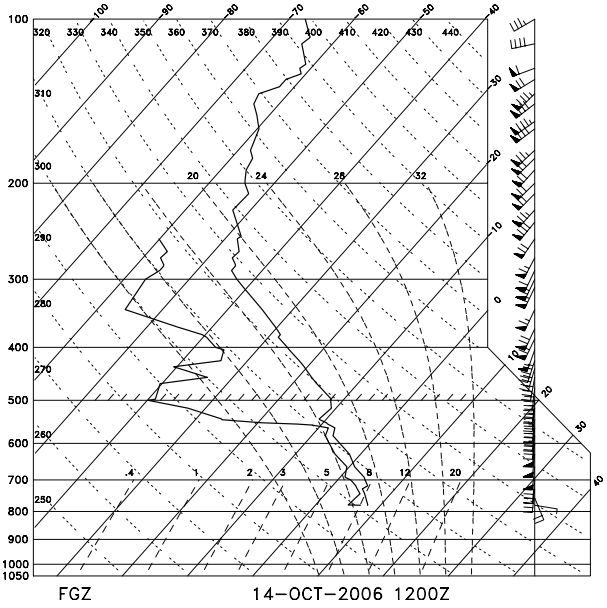


*Figure 10. As in Fig. 9 except at 1200 UTC 14 October 2006.*

are comparable to the 3rd and 4th quartiles of tornadic environments discussed by RB98. These should be considered strong contributing factors to the development of rotating storms with the potential for tornadoes.

The results presented here are similar to those of Monteverdi and Quadros (1994; hereinafter M94) and Monteverdi et al (2003; hereinafter M03) for central and northern California tornadoes, and Hanstrum et al. (2002; hereinafter H02) in their comparison of California and Australian tornadoes. In all of these studies, it was noted that CAPE was small but shear was large and even comparable to shear observed with springtime severe storms of the central Plains.

The results of M94, M03, H02, Blanchard (2006), and the present study suggest that large instability is not a requirement for the development of tornadoes if adequate deep-layer shear is also present. As noted by M03, "...the inference to be made is that there are various combinations of buoyancy and shear that permit supercell tornadogenesis. In low-buoyancy environments in which the deeper-layer shear is sufficient for supercells, vertical perturbation pressure gradient forces related to low-level shear are significant in augmenting the updraft..."

These results, however, are not inconsistent with those of Johns and Doswell (1992) and RB98 in which tornadic supercell thunderstorms have been observed in low buoyancy-high shear cases with CAPE less than 500 J $kg^{-1}$ and SRH greater than 200 $m^2$ $s^{-2}$. The events shown here represent one end of the CAPE and shear spectrum discussed by Johns and Doswell (1992) and RB98.

The low-buoyancy, high shear environment shares some similarities with tornadic supercells in a tropical cyclone environment (McCaul 1991; McCaul and Weisman 1996; McCaul and Weisman 2001). In their results, they noted the environment could support these

types of storms when both the buoyancy and shear are concentrated in the lower troposphere, a characteristic noted in the soundings shown in Figs. 9 and 10.

The results presented here provide additional evidence in support of the argument that shear may be at least as important as instability—and perhaps more so—and the warning forecaster must be vigilant for rotating thunderstorms with potential for tornadoes under a variety of instability/shear scenarios.

*Acknowledgments:* NCEP/NCAR Reanalysis data and images were provided by the NOAA/ESRL Physical Sciences Division, Boulder, Colorado, from their web site at http://www.cdc.noaa.gov/.

## REFERENCES

Adams, D.K. and A.C. Comrie, 1997: The North American Monsoon. *Bull. Amer. Met. Soc*., **78**, 2197–2213.

Blanchard, D. O., 2006: A cool season severe weather episode in northern Arizona. Preprints, *23rd Conf. on Severe Local Storms*, St. Louis, MO, Amer. Meteor. Soc.

Bluestein, H. B., 1993: Synoptic-Dynamic Meteorology in Midlatitudes. Vol. II, Observations and Theory of Weather Systems, Oxford University Press, 594 pp.

Kalnay, E. and Coauthors, 1996: The NCEP/NCAR Reanalysis 40-year Project. *Bull. Amer. Meteor. Soc*., **77**, 437–471.

Hales, J. E., Jr., 1985: Synoptic features associated with Los Angeles tornado occurrences. *Bull. Amer. Met. Soc.*, **66**, 657–662.

Hanstrum, B. N., G. A. Mills, A. Watson, J. P. Monteverdi, and C. A. Doswell III, 2002: The cool season tornadoes of California and southern Australia. *Wea. Forecasting*, **17**, 705–722.

Johns, R. H., and C. A. Doswell III, 1992: Severe local storms forecasting. *Wea. Forecasting*, **7**, 588–612.

McCaul, E. W., Jr., 1991: Buoyancy and shear characteristics of hurricane-tornado environments. *Mon. Wea. Rev*., **119**, 1954 –1978.

——, and M. L. Weisman, 1996: Simulations of shallow supercell storms in landfalling hurricane environments. *Mon. Wea. Rev*., **124**, 408– 429.

——, and ——, 2001: The sensitivity of simulated supercell structure and intensity to variations in the shapes of environmental buoyancy and shear profiles. *Mon.Wea.Rev*., **129**, 664–687.

Miller, R. C., 1972: Notes on analysis and severe-storm forecasting procedures of the Air Force Global Weather Central. Air Weather Service Tech. Rep. 200 (Rev.), 184 pp. [Available from Library, AFWA, Offutt AFB, NE 68113-5000; NTIS AD-744042.]

Monteverdi, J.P., and J. Quadros, 1994: Convective and rotational parameters associated with three tornado episodes in northern and central California. *Wea. Forecasting*, **3**, 285–300.

——, C.A. Doswell III, and G.S. Lipari, 2003: Shear parameter thresholds for forecasting tornadic thunderstorms in northern and central California. *Wea. Forecasting*, **18**, 357–370.

Rasmussen, E., and D. O. Blanchard, 1998: A baseline climatology of sounding-derived supercell and tornado forecast parameters. *Wea. Forecasting*, **13**, 1148–1164.

Schwartz, B. E., and M. Govett, 1992: A hydrostatically consistent North American radiosonde data base at the Forecast Systems Laboratory,1946–present. NOAA Tech. Memo. ERL FSL-4, 81 pp. [Available from the National Technical Information Service, 5285 Port Royal Road, Springfield, VA 22061.]

## Appendix

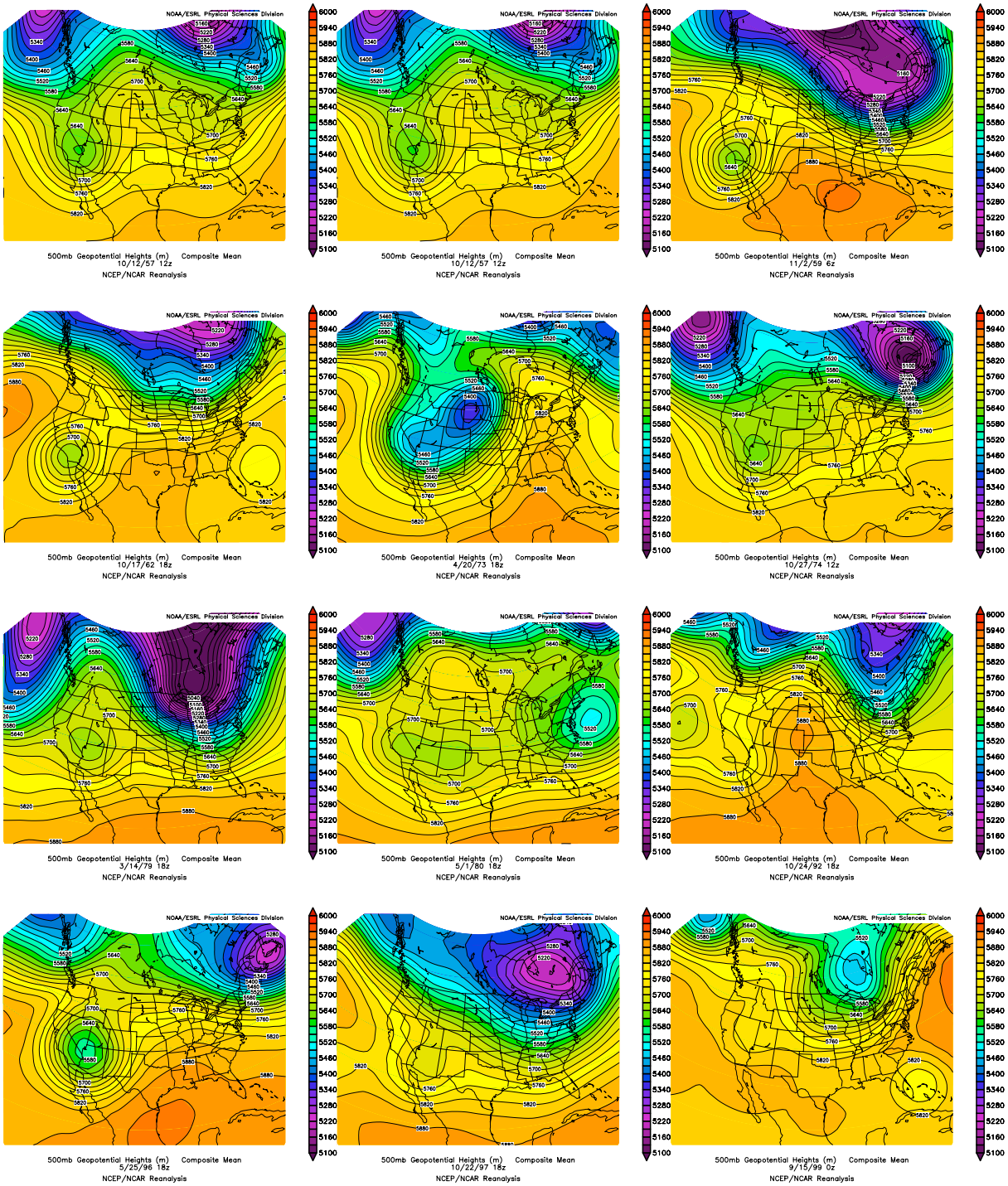


Figure A1: 500 mb height field analysis for each of the 19 closed low tornadic events.

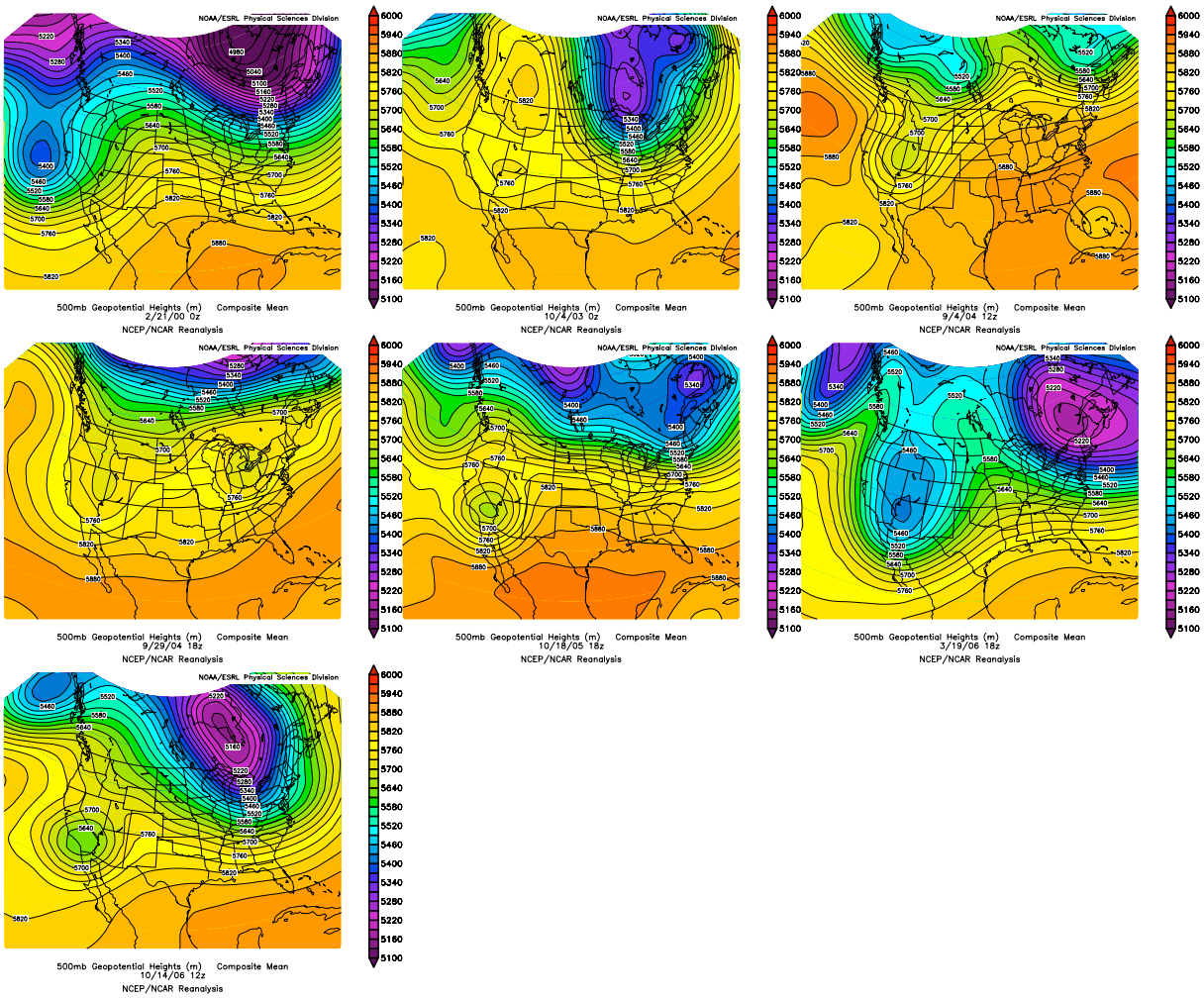


Figure A1 (cont.).